THE ROLE OF MANIPULATOR CHARACTERISTICS IN SELECTING THE IDEAL "EFFECTIVE VEHICLE"

By Ronald A. Hess

NASA Ames Research Center

SUMMARY

A structural model of the human pilot has been introduced and discussed in recent Manual Control Conferences. The model has been used to provide a rationale for certain nonlinear pilot control behavior such as stick pulsing and has served as a framework for studying aspects of motor skill development. In light of the theoretical background provided by the model, some past empirical pilot response phenomena are analyzed and shown to be attributable to manipulator or control stick characteristics. In particular, some recent problems associated with pilot/vehicle performance in glideslope tracking in short-takeoff and landing (STOL) aircraft are analyzed. The apparent contribution of the cockpit manipulator (throttle) characteristics to these problems are outlined and a solution proposed and evaluated in both simulation and flight test.

INTRODUCTION

In order to actively control some physical system such as an aircraft or automobile, the human operator must utilize a manipulator such as a control stick or steering wheel. The characteristics of the manipulator can have a profound effect upon the performance of the man-machine system. Although studies such as those by Herzog[1] and Merhav and Ya'Acov[2] have capitalized upon this interface to improve tracking performance in certain compensatory tasks, the specific inclusion of manipulator characteristics has not been a primary concern of the analyst. In pilot modeling, for example, the human has generally been treated as a servomechanism with zero output impedance. If the dynamics of the manipulator are significant in the frequency range of interest for manual control (typically $0.1 < \omega < 10$ rad/sec), they are usually lumped into those of the controlled element. Proprioceptive feedback has been postulated to fulfill a relatively minor role in determining overall pilot input-output characteristics although its contribution to the operation of the particular neuromuscular system operating the manipulator has been recognized as extremely important.[3]

Recently, Hess[4-7] has introduced and discussed what can be called a structural model of the human pilot in which proprioceptive feedback plays an important role in determining pilot equalization. In the next section,

this model will be discussed briefly and the implication of its structure as regards manipulator characteristics will be treated. With the model serving as a theoretical framework, some specific empirical examples of manipulator effects will then be discussed.

THE STRUCTURAL MODEL

The structural model of the human pilot proposed by Hess has been discussed at some length in the literature[4-7] and hence will only be outlined here. Figure 1 is a block diagram of this model for compensatory tracking behavior. The model of Fig. 1 has been divided into "central nervous system" and "neuromuscular system" components, a division intended to emphasize the nature of the signal-processing activity involved. System error e(t) is presented to the pilot via a display with dynamics Y_{de}. The rate of change of the displayed error is assumed to be derived from $e_d(t)$. The process of deriving error-rate is assumed to entail a computational time delay of τ_1 seconds. Constant gains K_e and $K_{\dot{e}}$ multiply the signals $e_d(t)$ and $e_d(t-\tau_1)$, respectively. The switch allows either of these two signals to be used as driving signals to the remainder of the model. A discussion regarding the utility of error-rate control is provided in Ref. 6. The action of the switch is parameterized by the variable P_1, which represents the probability that the switch will be in position 1 (error-rate control) at any instant of time. A central time delay of τ_0 seconds is included to account for the effects of latencies in the visual process sensing $e_d(t)$, motor nerve conduction times, etc. The resulting signal $u_c(t)$ provides a command to a closed-loop system, which consists of a model of the open-loop neuromuscular dynamics of the particular limb driving the manipulator, Y_{p_n}, and elements Y_f and Y_m, which emulate, at least approximately, the combined effects of the muscle spindles and the dynamics associated with higher level signal processing. A colored noise $n_u(t)$ is injected at the pilots's output as remnant.

As pointed out in Ref. 6, the signal $u_m(t)$ is really proportional to the time rate of change of vehicle output due to control activity, and as such, is a form of rate feedback. The first three rows of Table 1 show model parameters selected to give the describing function matches shown in Figs. 2-4. Table 2 shows the variation in pilot dynamics (in simplified form) with increases in the order of the controlled element dynamics. The third column shows the simplified form of the proprioceptive feedback implied by the combination of $Y_f Y_m$ in Fig. 1. For example, for $Y_c = K/s$, k=1, and from Fig. 1,

$$Y_f Y_m = K_1 s/(s + 1/T_1) \qquad (1)$$

For values of T_1 found appropriate for K/s dynamics ($T_1 \doteq 5$ secs from Table 1), $Y_f Y_m$ looks very much like a pure gain in the important region of open-loop crossover. Thus, row 2, column 3 of Table 2 shows the required proprioceptive feedback for controlling K/s dynamics to be applied force or displacement $u_\delta(t)$. This force or displacement is defined relative to a set-point or regulation point, e.g., the equilibrium position of a spring-

restrained control stick. K/s dynamics have long been associated with the most desirable "effective vehicle" characteristics for single-axis systems under manual control.[8] In terms of the classical servo-model of the human pilot (likened to column 2 of Table 2), a "pure-gain" pilot results, i.e., no pilot equalization is required. In terms of the structural model, which inherently contains two feedback loops, only feedback of proprioceptively sensed force or displacement is needed. The same cannot be said for $Y_c=K/s^2$. Here, k=2 and from Fig. 1

$$Y_f Y_m = K_1 s/(s + 1/T_1)(s + 1/T_2) \qquad (2)$$

For values of T_1 and T_2 found appropriate for K/s^2 dynamics ($T_1=T_2\doteq 2.5$ secs from Table 1) $Y_f Y_m$ looks very much like an integrator in the important region of crossover. Thus, row 3, column 3 of Table 2 shows the required proprioceptive feedback for controlling K/s^2 dynamics to be the integral of applied force or displacement from some set-point or regulation-point. A rationale for human operator pulsive control behavior was offered in Ref. 5 based upon the hypothesis that the human attempts to reduce the computational burden of time integration of $u_\delta(t)$ in higher levels of the central nervous system.

Lastly, consider $Y_c=K$, k=0 and, from Fig. 1,

$$Y_f Y_m = K_1(s + 1/T_2)s/(s + 1/T_1) \qquad (3)$$

With $T_1= T_2$, $Y_f Y_m$ takes the form of a differentiator. Thus, row 1, column 3 of Table 2 shows the required proprioceptive feedback for controlling K dynamics to be the time derivative of $u_\delta(t)$. Again, assuming the validity of the model of Fig. 1, this differentiation might also be accompanied by considerable activity in the higher levels of the central nervous system. Two things may mollify this situation, however. First, as Fig. 1 and Table 2 indicate, the pilot dynamics u_δ/e_d for this controlled element are a first order lag. This inherent filtering action of the error signal makes the pilot output $u_\delta(t)$ rather smooth and low frequency in nature. This is exemplified in Figs. 5 and 6 taken from Ref. 5 where the structural model was digitally simulated as part of a single-axis tracking task. Fig. 5 shows segments of $e_d(t)$ and $u_\delta(t)$ for $Y_c=K$ whereas Fig. 6 shows the same variables for $Y_c=K/s$. Notice the lower frequency content of $u_\delta(t)$ in Fig. 5 as opposed to that in Fig. 6. Second, the muscle spindles and Golgi tendon organs themselves, can provide direct rate information. This means that differentiation as an <u>operation</u> in the higher levels of the central nervous system may be obviated. Of special importance is the fact that the required proprioceptive feedback (or calculation) of du_δ/dt does <u>not</u> require information regarding a set-point or regulation point as was the case in the previous two controlled elements ($Y_c=K/s,K$). This will have important repercussions in the section which follows.

FLIGHT PATH CONTROL OF STOL VEHICLES

Reference 10 summarizes some interesting work, part of which involved the landing approach performance of a simulated powered-lift short takeoff and

landing (STOL) aircraft. Various vehicle dynamics were evaluated in piloted simulation. In the landing approaches, vertical flight path control was accomplished almost exclusively by throttle. In addition, very little column activity was needed for attitude/airspeed control. This was not accidental as an attitude-hold stability augmentation system (SAS) was designed and utilized for the express purpose of minimizing pilot activity with the longitudinal control column.

Figure 7 shows the dynamics of one of the configurations analyzed. The pertinent transfer function is

$$(d/\delta_T)' = (N^{\dot{d}}_{\delta_T})'/s\Delta' \qquad (4)$$

Here, d represents longitudinal vehicle motion perpendicular to the glideslope, and δ_T is throttle movement. The (') notation is meant to emphasize the fact that an inner attitude-loop is being closed by the SAS. No pilot inner-loop attitude closure is assumed, an assumption found to be valid from simulation. Table 3 lists the pertinent vehicle dynamics.

Figure 8 shows pilot/vehicle transfer function for the configuration of Fig. 7 measured at six frequencies around crossover. This "open loop" transfer function is of interest for four reasons: First, the crossover frequency appears to be somewhere between 0.3 and 0.4 rad/sec, a very low value for manual control experiments. Second, the pilot is not particularly successful in forcing the open-loop pilot/vehicle characteristics into a K/s-like form in the region of crossover. Third, the low frequency phase data exhibits none of the "phase droop"[6] normally associated with such pilot/vehicle open loop transfer function measurements. Finally, fitting this data with a simple lead-lag model would require an effective time-delay of 0.8 secs, quite a large value for manual control experiments.

We will now show that these four characteristics can be produced by the structural model of Fig. 1. Figure 9 shows the model-generated pilot/vehicle transfer function. The model parameters are listed in the fourth row of Table 1. The model fit was obtained by assuming that the pilot was controlling <u>rate</u> alone. This assumption was necessary to achieve an acceptable fit to the data. Actually, of course, the error-rate loop would serve as an inner-loop to an outer, error-loop closure. However, the fact that a reasonable fit to the data could be obtained by considering just error-rate control, alone, suggests that this control dominates. This is corroborated by experimental results from Ref. 10 where it was stated "All of the pilot's indicated that the technique for glideslope tracking was primarily to control glideslope deviation <u>rate</u> ($\dot{d}$)."

Using the structural model, we can now provide a rationale for this activity. The transfer function $(\dot{d}/\delta_T)'$ will exhibit pure-gain like characteristics for $\omega \leq 0.3$ rad/sec. Such characteristics have been hypothesized here to be ideal for manipulators which do not provide set-point information, such as the engine throttles used in Ref. 10. Normally, exclusive rate control would carry a workload burden imposed by the necessity of deriving rate information from displacement information. However, in the simulation of Ref. 10, rate information was available <u>directly</u>

from the Instantaneous Vertical Speed Indicator (IVSI) in the cockpit. Again, quoting from Ref. 10, the actual piloting technique was

"a. Keep $\dot{d}$ at a very low level by controlling IVSI with power, e.g., find a target IVSI that keeps the glideslope bug stationary on the display (nominally 800 ft/min)

b. If glideslope error (d) is diverging, try to first zero $\dot{d}$, than adjust power so d is slowly converging (i.e., pick a new target sink race on the IVSI).

c. If the glideslope error is less than one dot, make very small power adjustments (if any)."

Since rate information was available directly, the delay normally associated with rate derivation, τ_1 , was set to zero. To account for scanning delays, τ_0 was increased from the nominal 0.14 secs to 0.2 secs. Note that the model captures the salient features of the data including the four "anomolies" mentioned previously. In particular, note that no large time delays have to be hypothesized to match the phase lag data. It also appears that all of these anomolies have their origin in the characteristics of the manipulator and in the availability of explicit rate information.

Next, let us consider the results of an investigation reported in Ref. 11. In this study a flight test program was carried out to assess the feasibility of piloted instrument approaches along pre-defined, steep, curved and decelerating approach profiles in powered-lift aircraft operating on the backside of the power curve. Separate stability augmentation systems for attitude and speed were provided, as well as a supporting flight director and special electronic cockpit displays. Of particular interest was a problem encountered in glideslope tracking using a throttle flight director which produced K/s-like effective-vehicle characteristics in the frequency range $0.1 \leq \omega \leq 1.0$ rad/sec. Figure 10 shows the effective-vehicle characteristics (director+aircraft). Although the K/s dynamics do not extend beyond 1.0 rad/sec, no additional and deleterious phase lags accrue in this region. Figure 11 shows the oscillatory glideslope tracking characteristics revealed in flight tests for this configuration. The question now arises as to how the pilot would control this effective vehicle. Two obvious approaches are: 1) use rate control as in the previous example, 2) use displacement control. In the first case, the pilot's internal model of the effective vehicle in the frequency range $\omega \leq 1.0$ rad/sec would be a pure gain (k=0). According to the structural model, this would allow the manipulator to be suited to the dynamics. However, unlike the simulation just studied, rate information in the form of $\dot{\delta}_{TFD}$ (rate of change of throttle flight-director signal) is not explicitely available and would have to be derived by the pilot. Probable pilot/vehicle dynamics for this case are shown in Fig. 12. The structural model parameters are shown in the fifth row of Table 1. With the exception of τ_0 and τ_1 , they are identical to the parameters which yielded the match of Fig. 9, (fourth row of Table 1).

The value of τ_0 was increased from 0.2 to 0.5 secs to account for the fact that considerably more scanning probably occurred in the study reported

in Ref. 11 (a flight test) than in the one reported in Ref. 10 (a simulation). The value of τ_1 was increased from 0 to 0.2 secs to account for the fact that rate information had to be derived. As Fig. 12 indicates, stability margins are more than adequate. However, the necessity of continuously deriving rate information from the displayed flight-director signal δ_{TFD} may lead to high workload and inadequate time to control the remaining two directors and scan the status displays in the cockpit. In addition, rate control alone may not yield performance which the pilot deems acceptable.

Consider, on the other hand, the situation where the pilot controls displacement. Here, the pilot's internal model of the effective vehicle in the frequency range $\omega \leq 1.0$ rad/sec would be K/s (k=1). According to the structural model, the manipulator characteristics are not well suited to those of the effective-vehicle. It has been hypothesized here that the necessary proprioceptive information of applied force or displacement from a set-point (see Table 2) would not be available. Figure 13 shows the probable pilot/vehicle dynamics for this case under the preceding assumption. The model parameters are given in the sixth row of Table 1. They are closely related to those of the second row which utilized K/s dynamics. The most significant differences are the values of T_1 and τ_0. The rationale behind the revised value of τ_0 has just been given. For the sake of simplicity, no switching is assumed to occur, i.e., P_1=0. The decreased value of T_1 is intended to account for the assumption that little low-frequency proprioceptive feedback is available from the overhead throttles. This reduction means that the "break frequency" of the washout element Y_f of Fig. 1 is moved to higher frequencies, thus reducing the amount of low-frequency information available.

The effect of this change is rather dramatic as can be seen by comparing the phase angle plots of Figs. 12 and 13. Note the much larger phase lags apparent in Fig. 13. This lag increment is obviously not due to any changes in the delay τ_0, however. Rather, the closure of the two inner-loops of the structural model cause a real root to migrate to a position $s \doteq -0.4$. This is demonstrated in the two root locus diagrams for these closures shown in Figs. 14 and 15. Note from Fig. 13 that a closed loop instability is possible at ω=0.8 rad sec (0.13 cycles/sec). This is seen to compare quite favorably with the frequency of the path rate oscillations evident in Fig. 11. These oscillations constitute the glideslope tracking problem alluded to briefly at the beginning of our discussion of the experiments of Ref. 11. Although the oscillations of Fig. 11 represent a worst case example, they typified the glideslope tracking characteristics of the pilot/vehicle system. In Fig. 11, 5 cycles occur in approximately 38 secs (0.13 cycles/sec). The model results should not be interpreted as a "prediction" but rather as a rationale for the existence of a low frequency oscillation in the glideslope tracking for this effective-vehicle/manipulator combination. Note that in order to produce an unstable frequency at 0.8 rad/sec using a crossover model of the pilot,[8] an effective time delay on the order of 1.5 secs would have to be hypothesized!

From what has been discussed thus far, a solution to the flight-path oscillation problem would appear to lie in changing the characteristics of

either the throttle or the effective vehicle. The latter course was chosen in Ref. 11 and the dynamics of the effective vehicle (director+aircraft) were changed from K/s to K. This was accomplished by feeding back washed-out throttle position to the director. The reader is referred to Ref. 11 for details. Figure 16 shows the modified effective vehicle dynamics. The roll-off at frequencies beyond 5 rad/sec is due to a first-order filter being implemented to smooth the director signal at high frequencies. Figure 17 shows the resulting flight test results with the modified director (note the change in scales in the ordinates between Figs. 11 and 17). Performance is improved rather dramatically. Quoting from Ref. 11:

> "During the limited flight evaluation of these alternative throttle flight director control laws, and during the course of gathering the simulator data, pilot commentary indicated very little tendency toward oscillatory glidepath tracking characteristics. The pilots were not aware of providing any compensation while tracking the throttle-director bar, and were able to easily null the flight-director command bar without overshoot, using what were frequently step-like throttle inputs as can be seen in figure 63 (our Fig. 17). Once a correction was made, attention could temporarily be diverted to other display-scanning tasks without large errors developing in the throttle-director bar"

CLOSING REMARKS

The research just discussed was intended to point out that "ideal" effective-vehicle dynamics for manual control systems can be dependent upon manipulator characteristics. A structural model of the human pilot described in Ref. 6 which incorporated explicit proprioceptive feedback was used as a framework for interpreting some simulation and flight test results. The model was able to match measured pilot transfer function data exhibiting "anomolous" characteristics and was able to provide a rationale for oscillatory pilot/vehicle behavior. Finally, the model suggested a successful approach for improving the glideslope tracking performance of the aircraft exhibiting the oscillatory behavior.

REFERENCES

1. Herzog, J. H., "Proprioceptive Cues and Their Influence on Operator Performance in Manual Control," NASA CR-1248, 1969.

2. Merhav, I. J., and Ya'Acov, O. B., "Control Augmentation and Work-Load Reduction by Kinesthetic Information from the Manipulator," IEEE Transactions on Systems, Man and Cybernetics, Vol. SMC-6, No. 12, Dec. 1976, pp. 825-835.

3. Magdaleno, R. E., and McRuer, D. T., "Experimental Validation and Analytical Elaboration for Models of the Pilot's Neuromuscular Subsystem in Tracking Tasks," NASA CR-1757, 1971.

4. Hess, R. A., "A Dual-Loop Model of the Human Controller, "Journal of Guidance and Control, Vol. 1, July-Aug., 1978, pp. 254-260.

5. Hess, R. A., "A Rationale for Human Operator Pulsive Control Behavior," Journal of Guidance and Control, Vol. 2, May-June 1979, pp. 221-227.

6. Hess, R. A., "A Structural Model of the Adaptive Human Pilot," Journal of Guidance and Control, Vol. 3, No. 5, Sept.-Oct. 1980, pp. 416-423.

7. Hess, R. A., "Pursuit Tracking and Higher Levels of Skill Development in the Human Pilot," IEEE Transactions on Systems, Man, and Cybernetics, April 1981.

8. McRuer, D., "Human Dynamics in Man-Machine Systems," Automatica, Vol. 16, No. 3, May 1980, pp. 237-253.

9. Granit, R., The Basis of Motor Control, Academic Press, London and New York, 1970.

10. Holt, R. H., Craig, S. J., and Ashkenas, I. L., "Identification of Minimum Acceptable Characteristics for Manual STOL Flight Path Control," Federal Aviation Administration, FAA-RD-75-123, June 1976.

11. Hindson, W. A., Hardy, G. H., and Innis, R. C., "Flight-Test Evaluation of STOL Control and Flight-Director Concepts in a Powered-Lift Aircraft Flying Curved Decelerating Approaches," NASA Technical Publication 1641, 1981.

Table 1. Structural Model Parameter Values

Controlled-element dynamics	Model parameters											
	k	K_e	K_e'	K_2	P_1	T_1	T_2	K_1	τ_0	τ_1	ζ_n	ω_n
K	0	11.1	2.13	2.0	0.05	5.0	5.0	1.0	0.14	0.2	0.707	10.0
K/s	1	22.2	3.42	2.0	0.05	5.0	-	1.0	0.14	0.2	0.707	10.0
K/s^2	2	26.2	10.50	10.0	0.20	2.5	2.5	1.0	0.14	0.2	0.707	10.0
$(d/\delta_T)'$	0*	0.0	87.50	50.0	1.00	2.0	0.5	1.0	0.20	0.0	0.707	10.0
δ_{TFD}/δ_T	0*	0.0	87.50	50.0	1.00	2.0	0.5	1.0	0.50	0.2	0.707	10.0
δ_{TFD}/δ_T	1	0.77	0.0	10.0	0.00	0.2	-	1.0	0.50	-	0.707	10.0

*Internal model appropriate for rate tracking

Table 2. The Adaptive Pilot

Controlled Element		Simplified pilot dynamics	Required proprioceptive feedback
Y_c	k	Y_p	
K	0	$K_p e^{-\tau e s}/(T_I s + 1)$	$du_\delta(t)/dt$
K/s	1	$K_p e^{-\tau e s}$	$u_\delta(t)$
K/s^2	2	$K_p(T_L s + 1)e^{-\tau e s}$	$\int u_\delta(t)dt$

Table 3. STOL Configuration AP1 (Ref. 10)

V_0 (kts)	75.0
γ_0 (deg)	-6.0
θ_0 (deg)	1.87
δ_{T_0} (%)	30.6
Δ'	$(s + .25)(s + .36)(s + .67)(s + 8.32)(s^2 + 2(.5)(.33)s + .33^2)$
$(N^{\dot{d}}_{\delta_T})'$	$0.167(s + .475)(s + 1.75)(s + 8.3)(s^2 + 2(.99)(.163)s + .163^2)$

Prime notation indicates inner attitude-loop closed by SAS

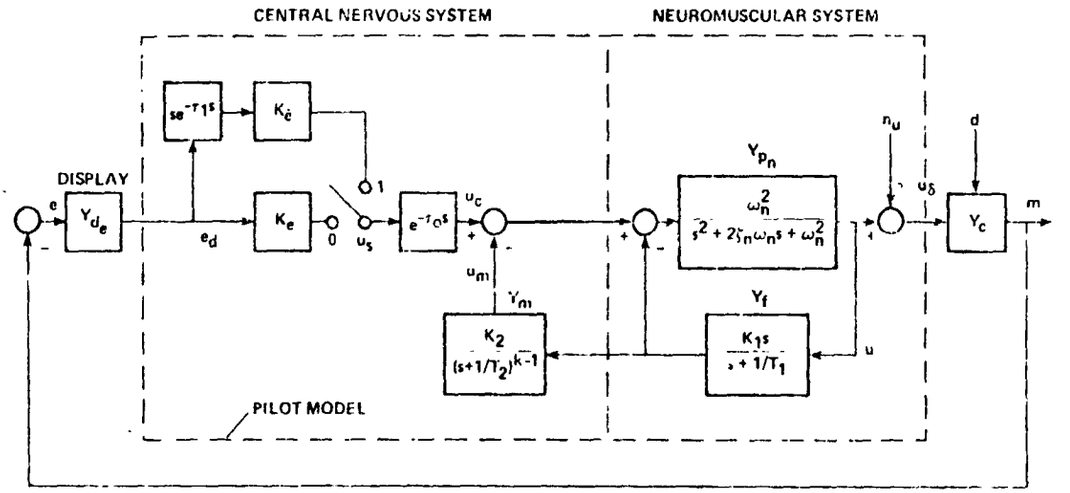

Figure 1. The structural model of the human pilot

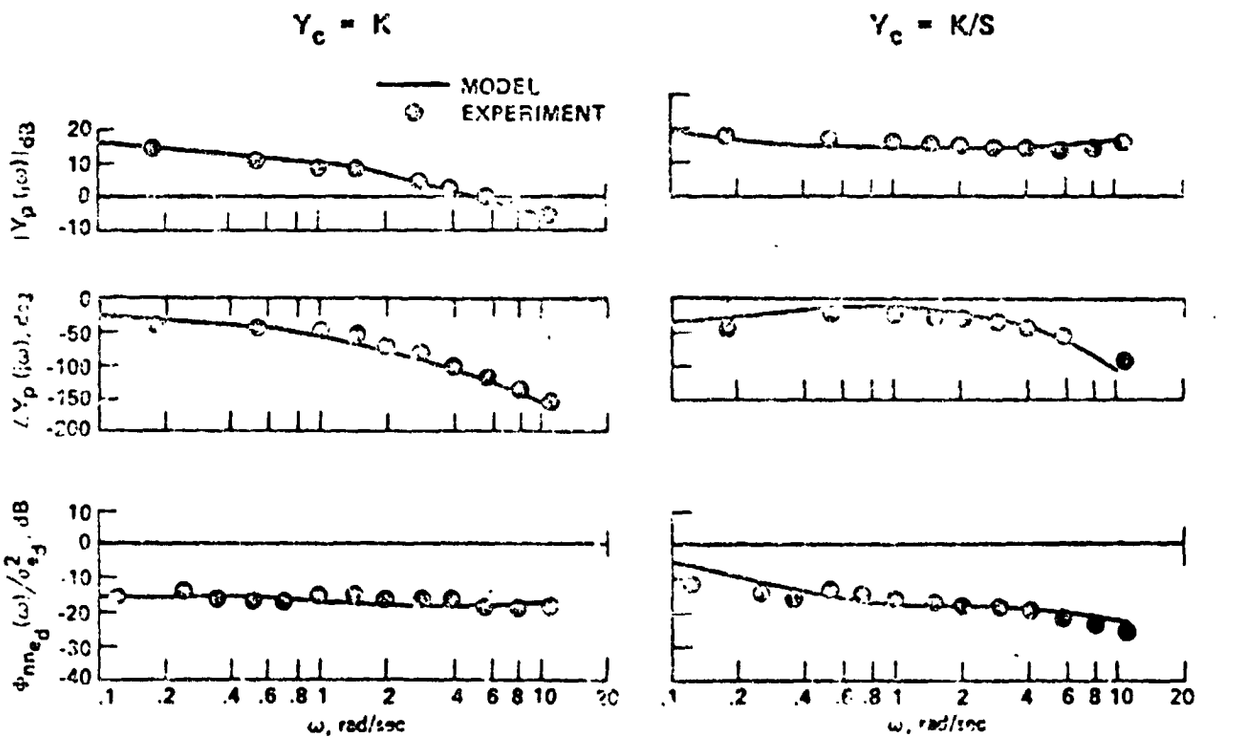

Figure 2. Describing function and remnant comparison, K controlled-element dynamics

Figure 3. Describing function and remnant comparison, K/s controlled element dynamics

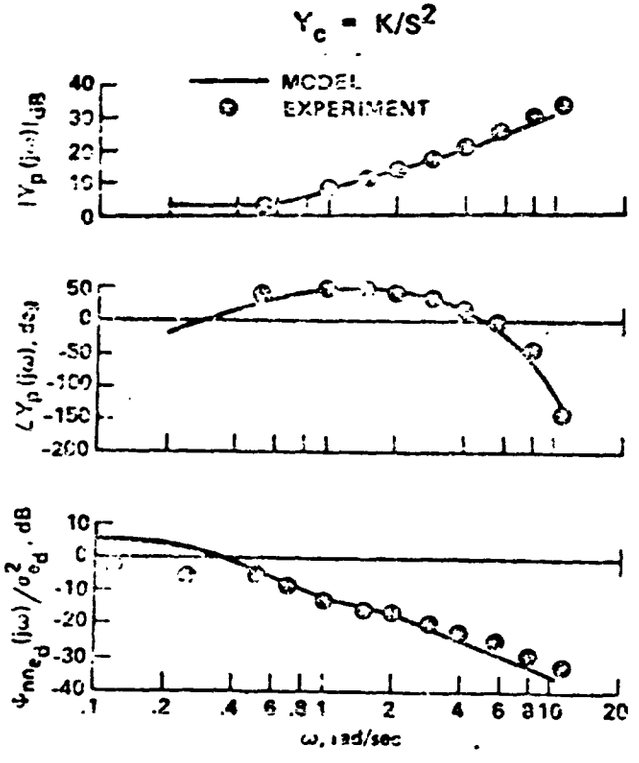

Figure 4. Describing function and remnant comparison, K/s^2 contolled-element dynamics

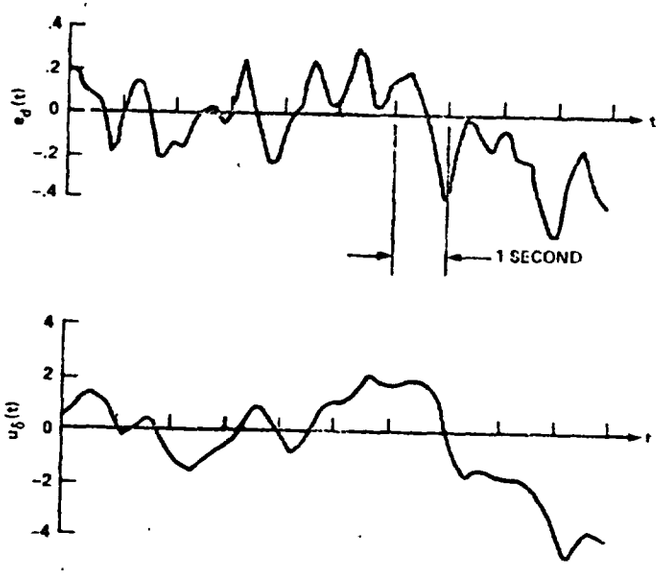

Figure 5. Error and control from structural model, K controlled-element dynamics

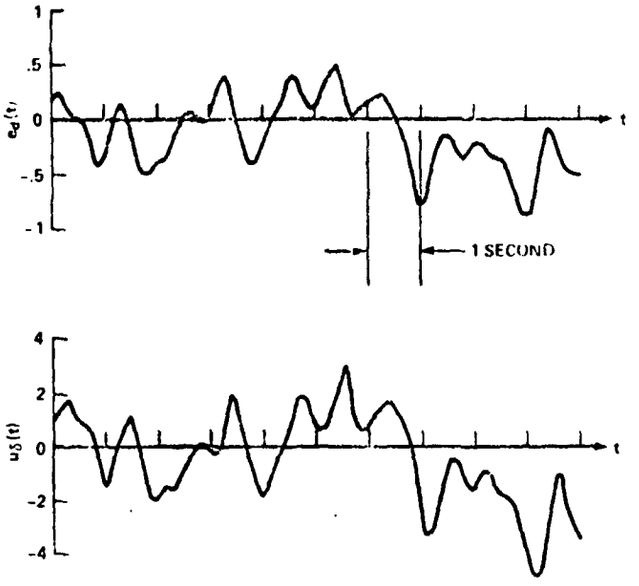

Figure 6. Error and control from structural model, K/s controlled-element dynamics

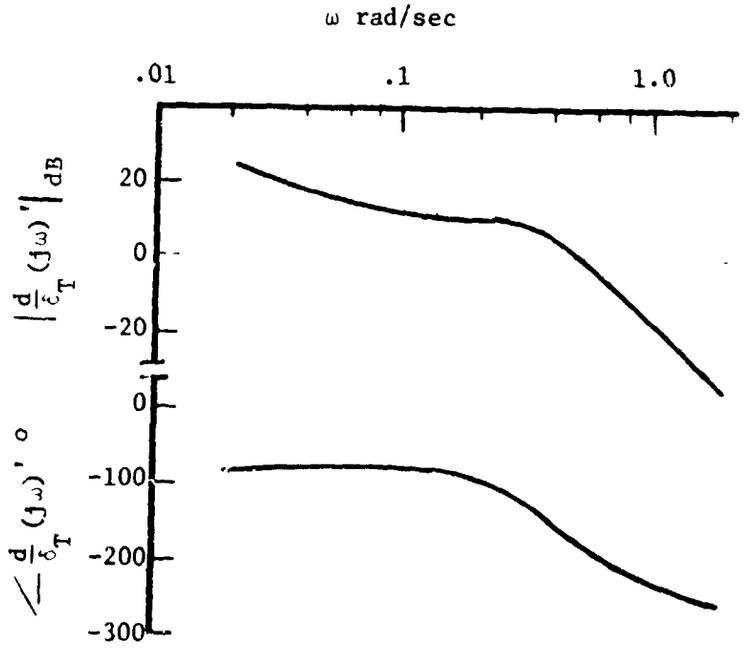

Figure 7. Vertical flight path to throttle characteristics for config. AP1 from Ref. 10

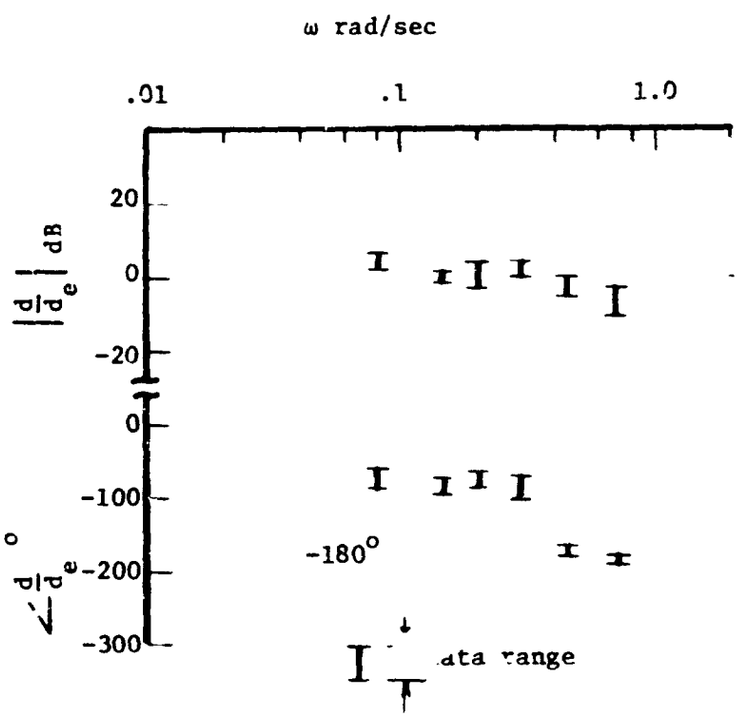

Figure 8. Measured pilot/vehicle transfer function for config. AP1 from Ref. 10.

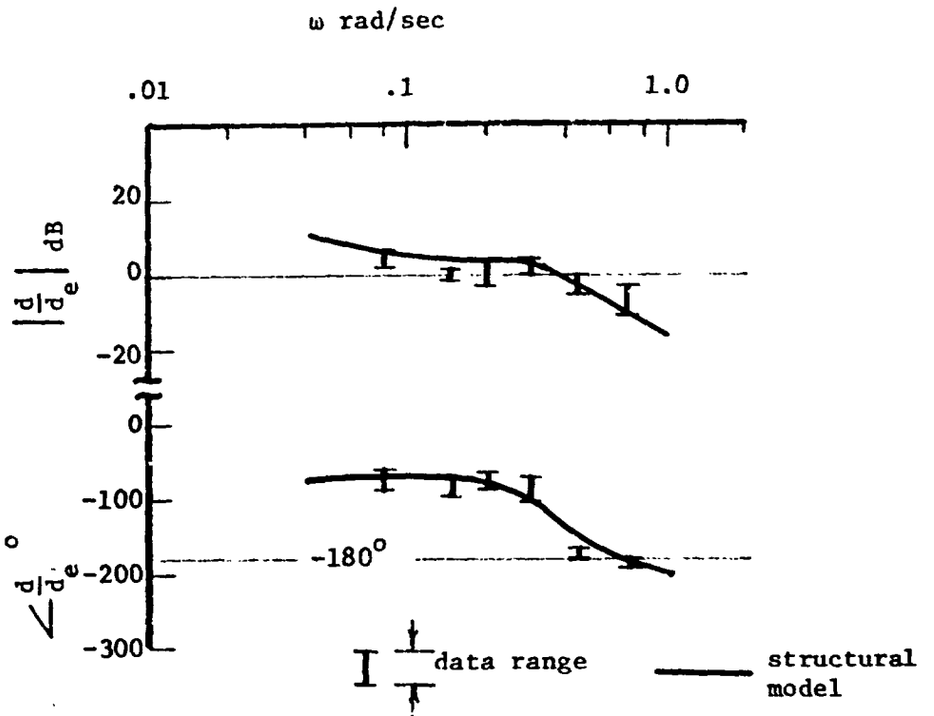

Figure 9. Comparison of experimental and model-generated transfer functions for config. AP1 from Ref. 10

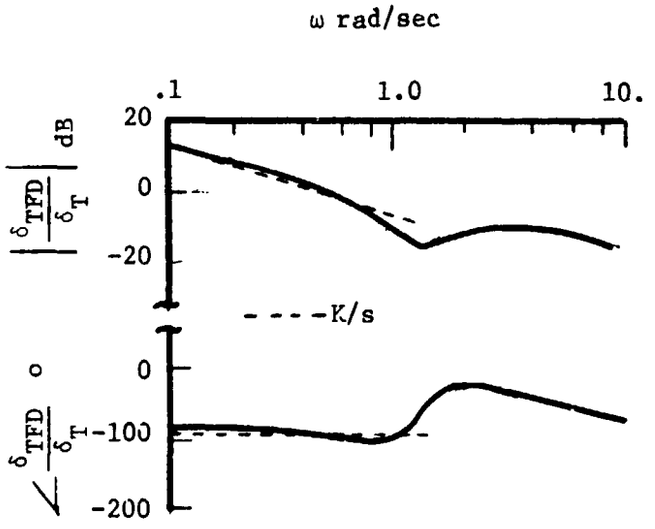

Figure 10. Effective vehicle (director+aircraft) for throttle control from Ref. 11

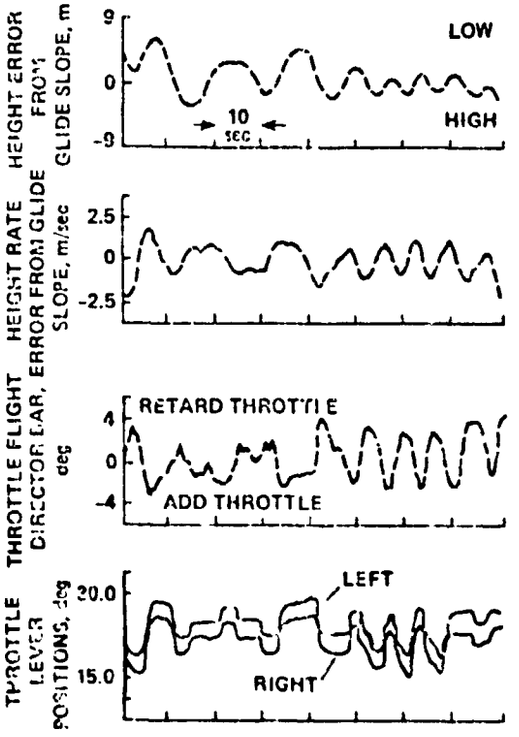

Figure 11. Glideslope tracking characteristics of aircraft from Ref. 11

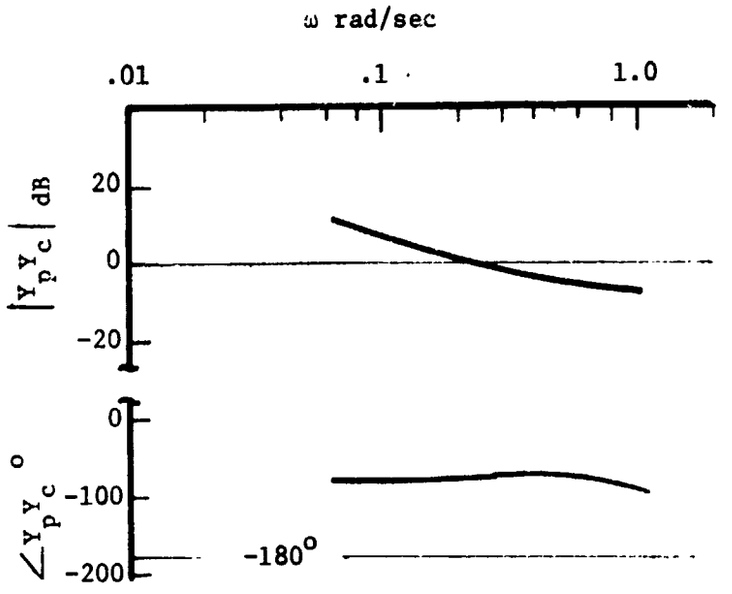

Figure 12. Model-generated transfer function for rate control of effective vehicle of fig. 10

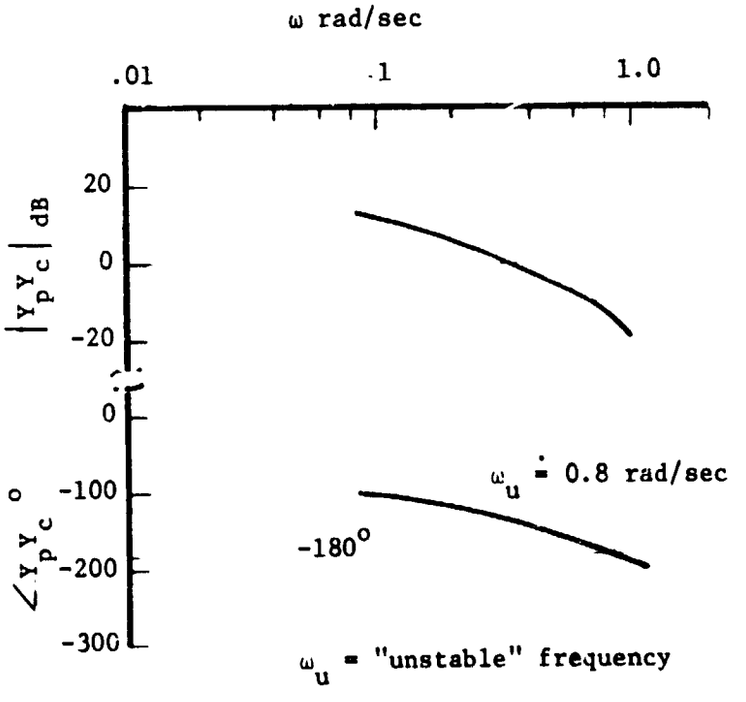

Figure 13. Model-generated transfer function for displacement control of effective vehicle of fig. 10

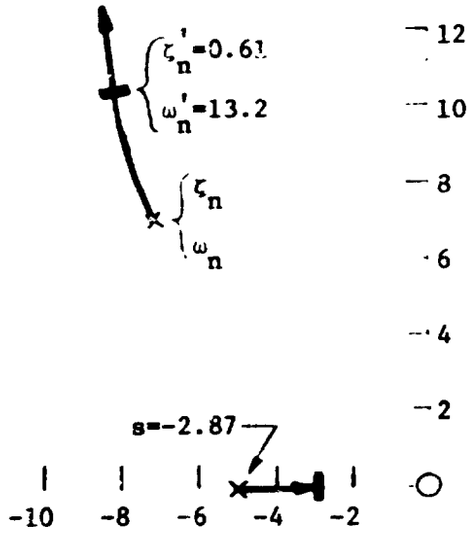

Figure 14. Root locus diagram for structural model inner-loop closure, model characteristics shown in fig. 13

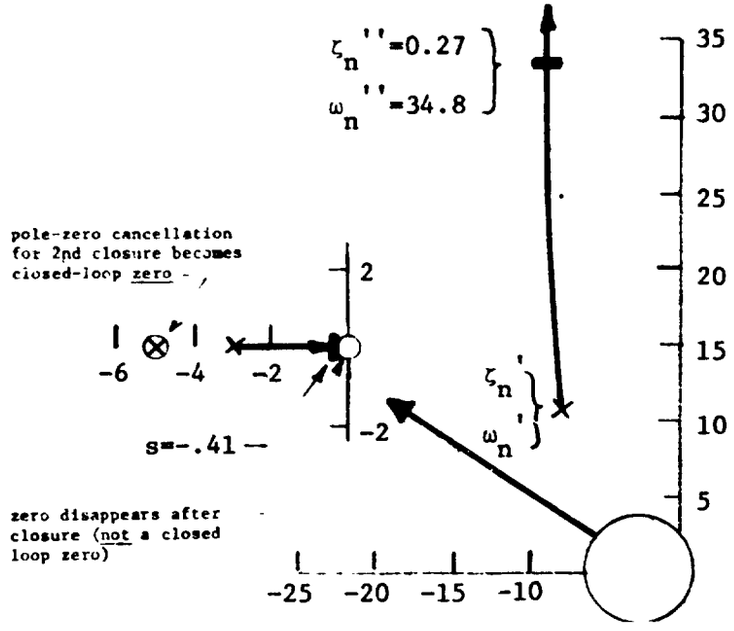

Figure 15. Root locus diagram for structural model outer-loop closure; model characteristics shown in fig. 13

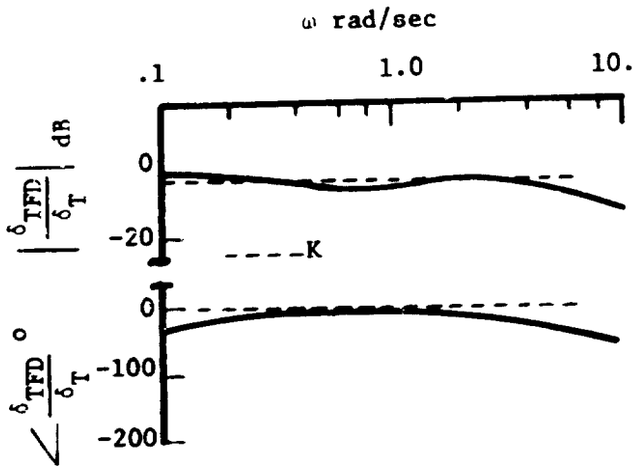

Figure 16. Modified effective vehicle (director+aircraft) for throttle control from Ref. 11

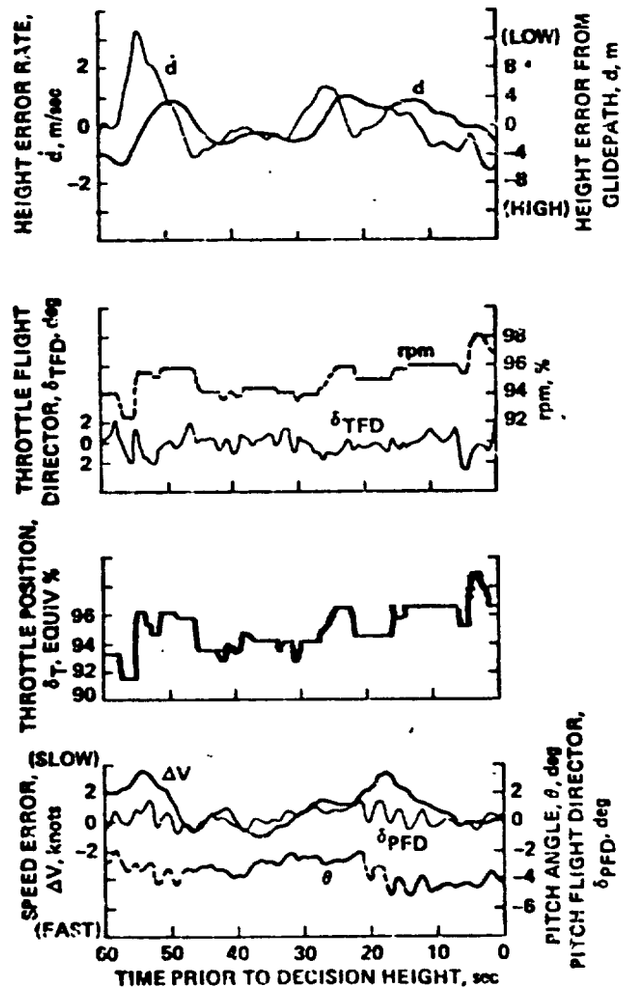

Figure 17. Glideslope tracking characteristics of aircraft with modified flight director from Ref. 11